# Analytic Solution for Adsorber Breakthrough Curves with Bidisperse Sorbents (Zeolites)

A time-domain solution in the form of infinite series for the breakthrough curves is derived for zeolite adsorbers. Three diffusion steps are accounted for in the solution: external film, macropore, and micropore. The solution is based on the assumption that the concentration profiles in micropores and macropores are both parabolic.

Based on the analytic solution, a simple criterion is given for the relative importance of the three individual mass transfer resistances. The adsorber behavior is determined by four independent dimensionless parameters. For the commercial zeolite sorbents, the bed behavior is dominated by two parameters: Henry's law constant ($K$) and the parameter $M_2$, which is the product of the stoichiometric time ($L/v$) and the time constant for macropore diffusion ($D_p/R_o^2$).

The analytic solution is in good agreement with experimental data for the breakthrough curves of nitrogen and methane carried in helium in 5A zeolite beds. When reduced to monodisperse pores, the solution is also in good agreement with Rosen's exact solution.

**P. L. Cen, R. T. Yang**
Department of Chemical Engineering
State University of New York
Buffalo, NY 14260

## Introduction

Adsorption has become increasingly important as a separations tool in the chemical and petrochemical industries. The degree of separation that can be achieved depends on the sharpness of the concentration wave front, also referred to as the mass transfer zone. The sharpness of the concentration front is measured by the breakthrough curve. The breakthrough curve is usually defined as the effluent concentration at the outlet of an initially clean bed subjected to an influent of constant concentration. The analogy is valid for chromatography, where the influent is a pulse or Dirac delta function of the adsorbate concentration.

For monodisperse sorbents, analytic solutions for the breakthrough curves have been derived for various mass transfer resistances, a few of which are mentioned below. Walter (1945a, b) and Furnas (1930) obtained solutions by considering only the external film resistance. Solutions were derived for intraparticle diffusion resistance by Thomas (1944) and by Edeskuty and Amundson (1952). Rosen's (1952, 1954) solution included both intraparticle diffusion and film diffusion. The solutions of Masamune and Smith (1965) included a finite rate for the surface step in addition to the intraparticle diffusion and external film resistances.

Although most of the commercial sorbents may be considered as having a monodisperse pore structure, zeolite molecular sieve is clearly an exception. The zeolite sorbent consists of small crystals, of sizes ranging approximately from 1 to 9 microns, which are pelletized with a small amount of binder. Thus, two distinct types of pores exist: micropores in the crystals and macropores in the binder. Because the time constants for diffusion (diffusivity/radius squared) are of the same order of magnitude for both types of pores, both must be considered in adsorber calculations. Ruckenstein et al. (1971) derived a solution for the uptake curve. Haynes (1975) obtained a solution for the chromatographic response in which the time-domain solution, or the inverse Laplace transform, must be solved numerically. Time-domain solutions were obtained by Friedrich et al. (1979) for a pulse input and by Rasmuson (1982) for a step input. Both of these solutions are in the integral form, and are very complicated indeed. A solution similar in form was also derived earlier by Kawazoe and Takeuchi (1974). All of the solutions (Ruckenstein et al.; Haynes; Friedrich et al.; Rasmuson; Kawazoe and Takeuchi) accounted for macropore, micropore, and film diffusion. Axial dispersion was also included in some derivations (Haynes; Friedrich et al.; Rasmuson). In all of the above derivations, the following simplifying assumptions were made: isothermality, constant fluid velocity, and linear isotherm.

The derivation can be simplified substantially if the intraparticle concentration profile is assumed to be parabolic. For the monodisperse pore structure, a solution in the form of infinite

series was derived by Liaw et al. (1979). These authors showed that the parabolic concentration profile assumption leads directly to Glueckauf's (1955) linear driving force approximation, which is an excellent and useful approximation in adsorber calculations (Rice, 1982; Yang et al., 1985). The same assumption has been used to calculate the uptake rate for a single zeolite pellet (not in an adsorber), and compared with exact solutions (Do and Rice, 1986). The comparison is not applicable to adsorbers.

In this work, an analytic solution is obtained for the bidisperse sorbent by assuming a parabolic concentration profile in both crystal and pellet. The solution is in good agreement with experimental data. It also compares well with Rosen's solution when the micropore resistance in our solution is neglected. Furthermore, through the solution a simple criterion is given for defining the relative importance of the three mass transfer resistances in adsorbers.

## Theoretical

The simplifying assumptions are: isothermality, plug flow, and linear isotherm, $q = KC_c$. In addition, both the pellet and crystals are assumed to be spherical in shape.

The mass balance equation for the crystal is

$$\frac{\partial q}{\partial t} = \frac{D_c}{r^2}\frac{\partial}{\partial r}\left(r^2\frac{\partial q}{\partial r}\right) \tag{1}$$

with the following initial and boundary conditions:

$$q = 0 \quad \text{at} \quad t = 0, 0 < r < r_o, 0 < z < L \tag{1a}$$

$$\frac{\partial q}{\partial r} = 0 \quad \text{at} \quad r = 0, t > 0 \tag{1b}$$

$$q = KC_p \quad \text{at} \quad r = r_o, t > 0 \tag{1c}$$

The mass balance equation for the pellet is

$$\frac{\partial C_p}{\partial t} + \frac{1-\alpha}{\alpha}\frac{\partial \bar{q}}{\partial t} = \frac{D_p}{R^2}\frac{\partial}{\partial R}\left(R^2\frac{\partial C_p}{\partial R}\right) \tag{2}$$

where

$$\bar{q} = \frac{3}{r_o^3}\int_o^{r_o} qr^2dr = \frac{3}{r_o^3}\int_o^{r_o} KC_c r^2 dr = K\bar{C}_c$$

and the initial and boundary conditions are:

$$C_p = 0 \quad \text{at} \quad t = 0, 0 < R < R_o, 0 < z < L \tag{2a}$$

$$\frac{\partial C_p}{\partial R} = 0 \quad \text{at} \quad R = 0, t > 0 \tag{2b}$$

$$D_p\frac{\partial C_p}{\partial R} = k(C - C_{p,R=R_o}) \quad \text{at} \quad R = R_o, t > 0 \tag{2c}$$

The mass balance equation for the fixed bed is:

$$v\frac{\partial C}{\partial z} + \frac{\partial C}{\partial t} + \frac{1-\epsilon}{\epsilon}\frac{\partial \bar{\bar{q}}}{\partial t} = 0 \tag{3}$$

where the first overbar at $q$ indicates the average over the crystal and the second overbar indicates the average over the entire pellet, and is given by

$$\bar{\bar{q}} = \frac{3}{R_o^3}\int_o^{R_o}\bar{q}R^2dR = \frac{3}{R_o^3}\int_o^{R_o} K\bar{C}_c R^2 dR = K\bar{\bar{C}}_c$$

The initial and boundary conditions for the bed are:

$$C = 0 \quad \text{at} \quad t = 0, 0 < z < L \tag{3a}$$

$$C = C_o \quad \text{at} \quad t > 0, z = 0 \tag{3b}$$

In order to obtain a solution for Eqs. 1–3, the concentration profiles in the crystals and pellets are both assumed parabolic:

$$C_c = a_o + a_2 r^2 \tag{4}$$

$$C_p = a_1 + a_3 R^2 \tag{5}$$

After evaluating $a_o$ and $a_2$ in terms of $C_p$, $r_o$, and $\bar{C}_c$, Eq. 1 becomes

$$\frac{\partial \bar{C}_c}{\partial t} = \frac{15D_c}{r_o^2}(C_p - \bar{C}_c) \tag{6}$$

Similarly, $a_1$ and $a_3$ may be evaluated in terms of $R_o$, $C_{p,R=R_o}$, and $\bar{C}_p$, and the following is derived from Eq. 2 (Cen, 1985):

$$\frac{\partial \bar{C}_p}{\partial t} + \frac{1-\alpha}{\alpha}K\frac{\partial \bar{\bar{C}}_c}{\partial t} = \frac{15D_p}{R_o^2}\frac{1}{1+\dfrac{5D_p}{kR_o}}(C - \bar{C}_p) \tag{7}$$

The two governing equations, Eqs. 6 and 7, may be combined by expressing $\bar{C}_p$ in terms of $\bar{\bar{C}}_c$ from Eq. 6,

$$\frac{\partial \bar{C}_p}{\partial t} = \frac{r_o^2}{15D_c}\frac{\partial^2 \bar{\bar{C}}_c}{\partial t^2} + \frac{\partial \bar{\bar{C}}_c}{\partial t} \tag{8}$$

to yield

$$\frac{\partial^2 \bar{\bar{C}}_c}{\partial t^2} + \left[1 + \frac{1-\alpha}{\alpha}K + \frac{(D_p/R_o^2)/(D_c/r_o^2)}{1+5D_p/(kR_o)}\right]\frac{15D_c}{r_o^2}\frac{\partial \bar{\bar{C}}_c}{\partial t} = \frac{(15D_c/r_o^2)(15D_p/R_o^2)}{1+5D_p/(kR_o)}(C - \bar{\bar{C}}_c) \tag{9}$$

The governing equations, Eqs. 1–3, are now reduced to two equations, Eqs. 9 and 3. Their dimensionless forms are:

$$\frac{\partial^2 Y_c}{\partial \tau^2} + 2\beta\frac{\partial Y_c}{\partial \tau} = \gamma(Y - Y_c) \tag{10}$$

$$\frac{\partial Y}{\partial Z} + \frac{\partial Y}{\partial \tau} + \delta\frac{\partial Y_c}{\partial \tau} = 0 \tag{11}$$

with the initial and boundary conditions:

$$Y = Y_c = 0 \quad \text{at} \quad \tau = 0, 0 < Z < 1 \tag{12}$$

$$\frac{\partial Y_c}{\partial \tau} = 0 \quad \text{at} \quad \tau = 0, 0 < Z < 1 \tag{13}$$

$$Y = 1 \quad \text{at} \quad \tau > 0, Z = 0 \tag{14}$$

The dimensionless parameters are:

$$Y = C/C_o, \quad Y_c = \bar{\bar{C}}_c/C_o, \quad Z = z/L, \quad \tau = vt/L$$

$$2\beta = \frac{15D_c}{r_o^2}\left[1 + \frac{1-\alpha}{\alpha}K + \frac{(D_p/R_o^2)/(D_c/r_o^2)}{1 + 5D_p/(kR_o)}\right]\frac{L}{v}$$

$$\gamma = \frac{(15D_p/R_o^2)(15D_c/r_o^2)}{1 + 5D_p/(kR_o)}\left(\frac{L}{v}\right)^2$$

$$\delta = \frac{1-\epsilon}{\epsilon}K$$

Equations 10–14 can be solved by Laplace transform (Cen, 1985). The solutions are given below.
For $\tau > Z$

$$Y = 1 + \sum_{m=1}^{\infty}\left[\frac{A_2^m}{(m-1)!}\int_o^{\tau-Z}\lambda^{m-1}\exp(-A_1\lambda)d\lambda + \frac{B_2^m}{(m-1)!}(-1)^m\int_o^{\tau-Z}\lambda^{m-1}\exp(-B_1\lambda)d\lambda + \sum_{n=2}^{m-1}(-1)^n\frac{mn}{n!^2(m-n)!^2}A_2^{m-n}B_2^n\int_o^{\tau-Z} \cdot e^{-A_1\lambda}\int_o^{\lambda}\phi^{n-1}(\lambda-\phi)^{m-n-1}e^{(A_1-B_1)\phi}\,d\phi d\lambda\right] \tag{15a}$$

and

$$Y = 0 \quad \text{for} \quad \tau < Z \tag{15b}$$

Equation 15 is the solution for the bed profile. The only assumption made is that of parabolic concentration profiles in the crystal and in the pellet. However, as in all previous solutions, this equation is in the integral form and is difficult to use. Equation 10 can be further simplified to yield a simpler and more useful solution.

For zeolite adsorber systems, the value of $2\beta$ is of the order of unity or greater. The first time-derivative of the average adsorbate concentration is much greater than the second derivative. Thus, in Eq. 10,

$$\frac{\partial^2 Y_c}{\partial \tau^2} \ll 2\beta\frac{\partial Y_c}{\partial \tau} \tag{16}$$

and Eq. 10 is approximated by

$$\frac{\partial Y_c}{\partial \tau} = \psi(Y - Y_c) \tag{17}$$

where

$$\psi = \frac{2\beta}{\gamma} = \left(\frac{15D_p/R_o^2}{1 + \frac{5D_p}{kR_o}}\frac{L}{v}\right)^{-1} \cdot \left[1 + \frac{1-\alpha}{\alpha}K + \frac{(D_p/R_o^2)/(D_c/r_o^2)}{1 + \frac{5D_p}{kR_o}}\right] \tag{17a}$$

The solution for Eqs. 17 and 11 with the boundary conditions in Eqs. 12–14 can be obtained by using the Laplace transform. The solution is:
For $\tau > Z$:

$$Y = e^{-\beta\psi Z}\left[e^{-\psi(\tau-Z)}I_o(2\sqrt{\beta\psi^2(\tau-Z)Z}) + \psi\int_o^{\tau-Z}e^{-\psi\lambda}I_o(2\sqrt{\beta\psi^2\lambda Z})d\lambda\right] \tag{18}$$

For $\tau < Z$:

$$Y = 0 \tag{18a}$$

where $I_o$ is the Bessel function of zero order and first kind, or

$$I_o(x) = \sum_{k=0}^{\infty}\frac{(x/2)^{2k}}{(k!)^2}$$

Equation 18 can be expressed in a series form and integrated to yield:

$$Y = e^{-\psi[\tau - Z(1-\beta)]}\sum_{j=0}^{\infty}\frac{[\psi(\tau-Z)]^j}{j!}\sum_{k=0}^{j}\frac{(\beta\psi Z)^k}{k!} \quad \tau > Z \tag{19}$$

The adsorbate concentration profile can be obtained by solving Eqs. 17 and 19 to yield:

$$Y_c = e^{-\psi[\tau - Z(1-\beta)]}\sum_{j=0}^{\infty}\frac{[\psi(\tau-Z)]^{j+1}}{(j+1)!}\sum_{k=0}^{j}\frac{(\beta\psi Z)^k}{k} \quad \tau > Z \tag{20}$$

and

$$Y_c = 0 \quad \tau < Z \tag{20a}$$

## Comparison of Theory with Rosen's Solution

The bed profile solution, Eq. 19, may be compared with Rosen's (1952, 1954) exact solution. Rosen's solution, however, was derived for a monodisperse pore structure. A comparison can be made, therefore, by assuming film and macropore diffusion control in Eq. 19, i.e., by assuming an $\infty$ time constant for the crystals, $D_c/r_o^2 = \infty$. Under this condition, it can be shown that Eq. 19 is reduced to:

$$Y = \exp\left(-\frac{\frac{7.5S}{X} + 5}{\frac{1}{X} + \frac{5\nu}{3X}}\right)\sum_{j=0}^{\infty}\frac{\left(\frac{7.5S/X}{\frac{1}{X} + \frac{5\nu}{3X}}\right)^j}{j!} \sum_{k=0}^{j}\frac{\left(\frac{5}{\frac{1}{X} + \frac{5\nu}{3X}}\right)^k}{k!}; \quad \tau > X \tag{21}$$

where

$$X = \frac{3D_pKL}{R_o^2 v}\frac{1-\epsilon}{\epsilon}, \quad S = \frac{2D_p(t - L/v)}{R_o^2}, \quad \nu = \frac{3D_pK}{kR_o}$$

The results calculated from Eq. 21 have been compared with Rosen's solution, as tabulated by Rosen (1954). The agreement is satisfactory under a variety of conditions (Cen, 1985). The solutions given by Eqs. 19, 20, and 21 converge slowly. Approximately 80 terms are needed. The calculation can be carried out in a computer. The required computation is, nevertheless, substantially simpler than previous solutions.

## Parametric Analysis of Adsorber Breakthrough Curves

The solution for the bed profile, Eqs. 19 and 17a, reveals that the adsorber is characterized by the following four independent dimensionless parameters:

$$K, M_1\left(=\frac{D_p/R_o^2}{D_c/r_o^2}\right), \quad M_2\left(=\frac{15D_p}{R_o^2}\frac{L}{v}\right), \quad M_3\left(=\frac{5D_p}{kR_o}\right)$$

Equation 17a is accordingly,

$$\psi=\left(\frac{M_2}{1+M_3}\right)^{-1}\left(1+\frac{1-\alpha}{\alpha}K+\frac{M_1}{1+M_3}\right) \tag{17b}$$

From the solution, a simple criterion may be established on the relative importance of the three mass transfer steps.

If $M_3 \ll 1$, or the mass transfer coefficient $k$ is very large, the adsorber becomes macropore-micropore diffusion control.

If in addition to the condition $M_3 \ll 1$,

$$M_1 \ll 1+\frac{1-\alpha}{\alpha}K \tag{22}$$

the mass transfer in the adsorber is controlled by the macropore diffusion step.

The conditions for micropore (crystal) diffusion control are, in addition to $M_3 \ll 1$:

$$M_1 \gg 1+\frac{1-\alpha}{\alpha}K \tag{23}$$

The ranges of values for the four independent dimensionless parameters are given below for zeolite adsorbers under practical conditions:

$$M_1 = 10 \text{ to } 1{,}000$$
$$M_2 = 1 \text{ to } 10$$
$$M_3 = 0 \text{ to } 0.5$$
$$K = 10 \text{ to } 1{,}000$$

Based on the approximate solution (Eq. 19), the effects of the four parameters on the adsorber dynamics will be discussed. Briefly, the effects of $K$ and $M_2$ are most important, whereas $M_1$ and $M_3$ are not important. The following discussion is based on $Z = 1$, $\epsilon = 0.45$, and $\alpha = 0.26$, which are appropriate values for zeolite beds.

### *Effects of Henry's constant (K)*

The strong effects of Henry's constant on the breakthrough curves are shown in Figures 1 and 2, as calculated from Eq. 19.

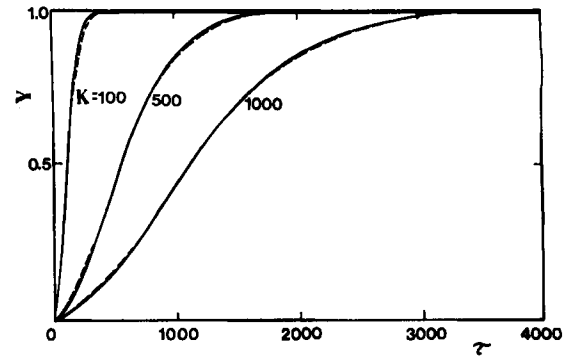


**Figure 1. Effects of Henry's constant on breakthrough curves.**
$M_2 = 1.0$; $M_3 = 0.1$; $M_1 = 10$ (—) or 1,000 (– – –).

As expected, a small $K$ value causes an early breakthrough. The figures also show that the breakthrough curves are more diffuse for higher $K$ values. These diffuse wave fronts can be sharpened by increasing the value of $M_2$. This is clearly shown by comparing Figures 1 and 2. For the same values of $M_1$, $M_3$, and $K$, all wave fronts are substantially sharpened by increasing $M_2$ from 1 to 3.

### *Effects of parameter $M_1$*

$M_1$ indicates the relative importance of micropore/macropore diffusion, i.e., a higher $M_1$ indicates a more important micropore resistance. Figure 3 shows that the parameter $M_1$ has only a minor effect on the breakthrough curves. The effects of $M_1$ under conditions other than that given in Figure 3 have also been calculated, but are not shown here. For $K = 1{,}000$, $M_2 = 2$, and $M_3 = 0$ as in Figure 3, the four curves shown in Figure 3 almost coincide. For smaller $K$ values, however, the effects of $M_1$ become more appreciable. This result indicates that micropore diffusion resistance becomes more important, as compared to macropore diffusion, only at low values of Henry's constant. This conclusion is in agreement with the observations of Ruthven and Loughlin (1972).

### *Effects of parameter $M_2$*

The predicted breakthrough curves are shown in Figures 4 and 5 for conditions pertaining to zeolite sorbent pellets. The

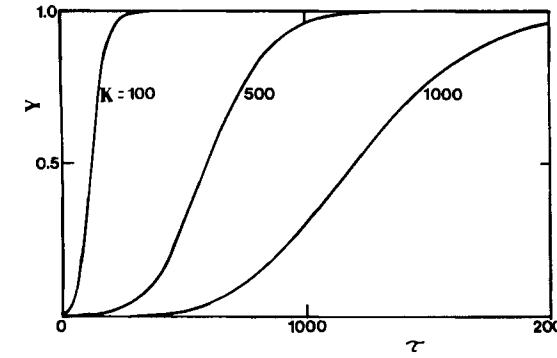


**Figure 2. Effects of Henry's constant on breakthrough curves.**
$M_1 = 10$, $M_2 = 3$; $M_3 = 0.1$.

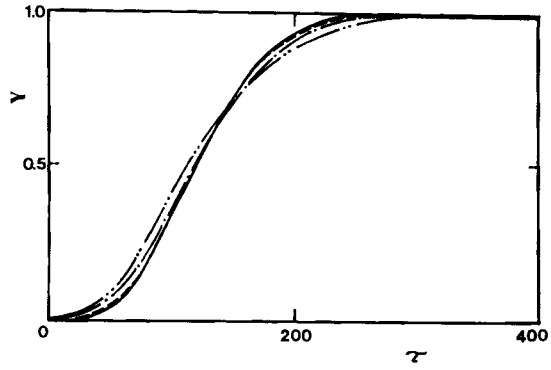


**Figure 3. Effects of parameter $M_1$ on breakthrough curves.**

$M_2 = 2$; $M_3 = 0$; $K = 100$; $M_1 = 0$ (—), 100 (----), 500 (— · —), 1,000 (— · · —).

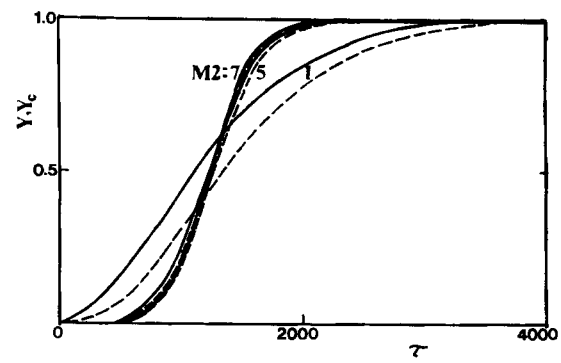


**Figure 5. Effects of parameter $M_2$ on breakthrough curves.**

$K = 1{,}000$; $M_1 = 10$; $M_3 = 0$.
— = $Y$; ---- = $Y_c$.

film resistance is negligible, or $M_3 = 0$, and the $M_1$ value is of the order 10.

Two important phenomena are predicted by the analytic solution, Eq. 19. First, the macropore (pellet) diffusion constant $D_p/R_o^2$ and the stoichiometric time $L/v$ are grouped together in a single independent parameter, $M_2$. Second, although under Henry's law regime (which is not a "favorable" isotherm), the concentration wave front is sharpened as the bed length or $M_2$ is increased for the sorbent with a bidisperse pore structure. Figures 4 and 5 further show that, similar to the case with a favorable isotherm, a constant pattern is reached as the bed length is further increased. Under the conditions studied here ($M_1 = 10$, $M_3 = 0$), the value of $M_2$ for reaching the constant pattern is approximately 5 (Figure 5). When the constant pattern is reached, the interparticle concentration $Y$ and the average concentration in the pellet, $Y_c$, should be nearly equal. ($Y_c$ is predicted from Eq. 20.)

### *Effects of parameter $M_3$*

The effects of $M_3$ on the breakthrough curves are minimal under a wide range of conditions. No figures will be shown here. The reason for the lack of influence by $M_3$ can be seen in Eq. 17a, where $M_3$ is present in both numerator and denominator.

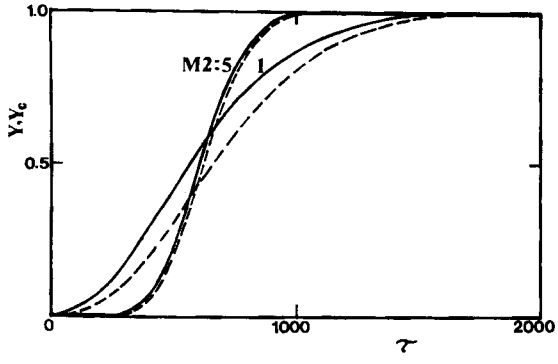


**Figure 4. Effects of parameter $M_2$ on breakthrough curves.**

$K = 500$; $M_1 = 10$; $M_3 = 0$.
— = $Y$; ---- = $Y_c$.

### *Desorption dynamics*

With the same assumptions made for adsorption, the bed profiles for desorption by inert gas purge can also be predicted. The boundary conditions are:

$$Y = Y_c = 1 \quad \text{at} \quad \tau = 0 \quad \text{and} \quad 0 < Z < 1 \tag{24}$$

$$Y = 0 \quad \text{at} \quad Z = 0, \tau > 0 \tag{25}$$

The solution is

$$Y = 1 - e^{-\psi[\tau - Z(1-\beta)]} \sum_{j=0}^{\infty} \frac{[\psi(\tau - Z)]^j}{j!} \sum_{k=0}^{j} \frac{(\beta\psi Z)^k}{k!} \tag{26}$$

Compared with Eq. 19, it is seen that the desorption curve is simply a mirror image of the adsorption curve.

## Comparison of Theory and Experiments

Breakthrough curves were measured in columns of 5A zeolite. The experimental conditions were designed such that accurate breakthrough curves were obtained while at the same time the assumptions made in the theory were met. The feed mixture concentration was sufficiently low that isothermality and constant flow velocity were nearly achieved. The column diameter was much greater than the particle size to ensure the absence of the effect by radial dispersion. The effect of axial dispersion was minimized by using a relatively high flow rate.

**Table 1. Adsorber Column Characteristics, 5A Zeolite Sorbent**

| | Column 1 | Column 2 |
|---|---|---|
| Inside dia., cm | 2.0 | 2.0 |
| Particle size | 1/16 in (1,587 $\mu$) | 40–60 U.S. mesh (250–420 $\mu$m) |
| Column height, cm | 35 | 35 |
| Interparticle porosity ($\epsilon$) | 0.475 | 0.525 |
| Intraparticle porosity ($\alpha$) | 0.330 | 0.330 |
| Crystal dia. ($2r_o$), $\mu$m | 3.5 | 3.5 |

Table 2. Conditions for Adsorber Breakthrough Experiments

| | Run Number | | | | |
|---|---|---|---|---|---|
| | 1 | 2 | 3 | 4 | 5 |
| Column number | 1 | 1 | 1 | 1 | 2 |
| Adsorptive gas | $N_2$ | $N_2$ | $N_2$ | $CH_4$ | $CH_4$ |
| He flow rate, cm/s | 5.55 | 5.55 | 3.23 | 5.55 | 5.55 |
| Feed conc. ($C_o$), % | 0.93 | 1.22 | 1.05 | 1.30 | 1.30 |
| $K$ | 39.36 | 39.36 | 39.36 | 23.90 | 23.90 |
| $D_p$, cm$^2$/s | 0.10 | 0.10 | 0.10 | 0.11 | 0.11 |
| $D_c \times 10^{11}$, cm$^2$/s | 8.75 | 8.75 | 8.75 | 47.0 | 47.0 |
| $k$, cm/s | 2,763.0 | 2,763.0 | 2,116.0 | 2,763.0 | 2,763.0 |

$T$ = 20°C, $P$ = 1 atm.

## *Experimental*

The sorbent was Linde 5A zeolite in two sizes: 1/16 in (1,587 μm) and 40–60 U.S. mesh (250–420 μm). Prior to the experiment, the sorbent was regenerated at 350°C for 12 h in helium flow. The breakthrough curves were measured at 20°C and 1 atm. The adsorptive gases were nitrogen and methane, as their isotherms and diffusivities had been measured. Helium was the carrier gas. All gases were purchased from Linde Specialty Gases, with the following guaranteed minimum purities: 99.0% for $CH_4$, 99.99% for $N_2$, and 99.995% for He. The inlet flow rates of the gases were controlled by mass flow meters (manufactured by Tylan Corporation). The effluent gas concentrations were measured by gas chromatography (GC). Samples were taken and stored with syringes equipped with locks, followed by GC analysis. The adsorber characteristics are shown in Table 1. The experimental conditions are summarized in Table 2.

## *Comparison between experimental data and theory*

Transport and isotherm data are given in Table 2. The micropore (crystal) diffusivities are taken from the measurements by Ruthven and Derrah (1972, 1975). The macropore diffusivities were calculated based on transition-regime diffusion with a mean pore diameter of 320 nm and a tortuosity factor of 4.0 (Ma and Ho, 1974). The film coefficients, $k$, were calculated based on an empirical correlation (Wakao and Funazkri, 1978). The Henry's law constants for methane and nitrogen were measured in this laboratory, since the literature values were either for the high-pressure range ($CH_4$) or differed widely ($N_2$).

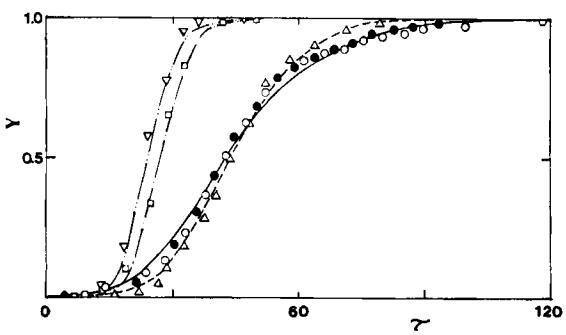


**Figure 6. Comparison of experimental data (symbols) and theory (curves) for $N_2$ and $CH_4$ breakthrough curves in 5A zeolite beds. ○ Run 1; ● Run 2; △ Run 3; □ Run 4; ▽ Run 5.**

The measured breakthrough curves are shown in Figure 6, as compared with the predictions by Eq. 19. The agreement between theory and experiment is fair.

The strong effects of Henry's constant were clearly shown by comparing the two adsorptive gases, i.e., comparing the two groups of curves: runs 1, 2, 3, and runs 4, 5. As predicted by theory, a lower Henry's constant also resulted in a sharper wave front.

Under the experimental conditions, $M_3 \ll 1$ and $M_1 \gg 1 + (1 - \alpha/\alpha)\ K$. Thus, the adsorber was micropore diffusion control. Under such conditions, it was predicted that the pellet size, or $M_1$, would have no or minimal effects on the breakthrough curves. This prediction was verified by a comparison between runs 4 and 5. The small shift between these two runs, Figure 6, was due to the different pellet sizes and hence different void spaces in the bed.

The effects of the parameter $M_2$ were shown in the comparison between runs 1 and 3. As predicted by the theory, a lower flow rate and hence a higher $M_2$ value (run 3) produced a sharper breakthrough curve.

The theory also predicts that the breakthrough curve, expressed in terms of $C/C_o$, is independent of $C_o$, the feed concentration. This was indeed verified by comparing the results of runs 1 and 2, Figure 6. No difference was detected for different feed concentrations. The effects of $M_3$ were not important due to the high value of the film mass transfer coefficient.

## Acknowledgment

This work was supported by the U.S. Department of Energy under Grant No. DE-AC21-85MC22060.

## Notation

$C_c$ = adsorbate concentration in crystal, kmol/m$^3$
$\bar{C}_c$ = average value of $C_c$ averaged over the crystal, kmol/m$^3$
$\bar{\bar{C}}_c$ = average value of $\bar{C}_c$ averaged over the pellet, kmol/m$^3$
$C$ = adsorbate concentration in fluid phase, kmol/m$^3$
$C_o$ = feed concentration, kmol/m$^3$
$C_p$ = adsorbate concentration in macropore, kmol/m$^3$
$\bar{C}_p$ = average value of $C_p$ averaged over the pellet, kmol/m$^3$
$D_c$ = diffusivity of adsorbate in crystal, m$^2$/s
$D_p$ = diffusivity of adsorbate in macropore, m$^2$/s
$k$ = mass transfer rate constant in fluid film, m/s
$K$ = Henry's constant
$L$ = column height, m
$M_1, M_2, M_3$ = dimensionless parameters
$q$ = adsorbed amount, kmol/m$^3$
$\bar{q}$ = average of $q$ over the crystal, kmol/m$^3$
$\bar{\bar{q}}$ = average of $\bar{q}$ over the pellet, kmol/m$^3$
$r$ = radial distance in crystal, m
$r_o$ = radius of crystal, m
$R$ = radial distance in pellet, m
$R_o$ = radius of pellet, m
$S$ = Rosen's dimensionless parameter
$t$ = time, s
$v$ = flow rate, m/s
$X$ = Rosen's dimensionless parameter
$Y$ = dimensionless concentration ($= C/C_o$)
$Y_c$ = dimensionless concentration
$z$ = axial distance in bed, m
$Z$ = dimensionless distance ($= z/L$)

### *Greek letters*

$\alpha$ = intrapellet void fraction
$\beta$ = dimensionless parameter
$\gamma$ = dimensionless parameter
$\delta$ = dimensionless parameter

$\epsilon$ = interpellet void fraction
$\tau$ = dimensionless time
$\psi$ = dimensionless parameter, Eq. 17a
$\nu$ = Rosen's parameter

## *Literature cited*


Cen, P. L., "A Study on Adsorber Breakthrough Curves and Multicomponent, Bulk Gas Separation," Ph.D. Diss., State Univ. New York, Buffalo (1985).

Do, D. D., and R. G. Rice, "Approximate Solutions for Batch Adsorbers Containing Adsorbents with Bidisperse Pore Structure," *Chem. Eng. Commun.*, (1986).

Edeskuty, F. J., and N. R. Amundson, "Mathematics of Adsorption. IV: Effect of Intraparticle Diffusion in Agitated Static Systems," *Ind. Eng. Chem.*, **44**, 1968 (1952).

Friedrich, S., C. Bode, and W. Flock, "Investigation of the Diffusion in Bidisperse Structured Catalysts by Gas Chromatography. A Note on Time-Domain Solution," *Chem. Eng. Sci.*, **34**, 418 (1979).

Furnas, C. C., "Heat Transfer from a Gas Stream to a Bed of Broken Solids," *Trans. AIChE*, **24**, 142 (1930).

Glueckauf, E., "Theory of Chromatography. 10: Formula for Diffusion into Spheres and Their Application to Chromatography," *Trans. Faraday Soc.*, **51**, 1540 (1955).

Haynes, H. W., "The Determination of Effective Diffusion by Gas Chromatography. Time-Domain Solutions," *Chem. Eng. Sc.*, **30**, 955 (1975).

Kawazoe, K., and Y. Takeuchi, "Mass Transfer in Adsorption on Bidisperse Porous Materials," *J. Chem. Eng. Japan*, **7**, 431 (1974).

Liaw, C. H., J. S. P. Wang, R. A. Greenkorn, and K. C. Chao, "Kinetics of Fixed-Bed Adsorption: A New Solution," *AIChE J.*, **25**, 376 (1979).

Ma, Y. H., and S. Y. Ho, "Diffusion in Synthetic Faujasite Powder and Pellets," *AIChE J.*, **20**, 279 (1974).

Masamune, S., and J. M. Smith, "Adsorption Rate Studies—Interaction of Diffusion and Surface Processes," *AIChE J.*, **11**, 34 (1965).

Rasmuson, A., "Time-Domain Solution of A Model for Transport Processes in Bidisperse Structured Catalysts," *Chem. Eng. Sci.*, **37**, 787 (1982).

Rice, R. G., "Approximate Solutions for Batch, Packed Tube, and Radial Flow Adsorbers—Comparison with Experiment," *Chem. Eng. Sc.*, **37**, 83 (1982).

Rosen, J. B., "Kinetics of a Fixed-Bed System for Solid Diffusion into Spherical Particles," *J. Chem. Phys.*, **20**, 387 (1952).

———, "General Numerical Solution for Solid Diffusion in Fixed Beds," *Ind. Eng. Chem.*, **46**, 1590 (1954).

Ruckenstein, E., A. S. Vaidyanathem, and G. R. Youngquist, "Sorption by Solids with Bidisperse Pore Structures," *Chem. Eng. Sc.*, **26**, 1305 (1971).

Ruthven, D. M., and R. I. Derrah, "Transition State Theory of Zeolite Diffusion—Diffusion of $CH_4$ and $CF_4$ in 5A Zeolite," *J. Chem. Soc. Trans. I.*, **68**, 2332 (1972).

———, "Diffusion of Monatomic and Diatomic Gases in 4A and 5A Zeolites," *J. Chem. Soc. Trans. I.*, **71**, 2031 (1975).

Ruthven, D. M., and K. F. Loughlin, "Diffusional Resistance of Molecular Sieve Pellets," *Can. J. Chem. Eng.*, **50**, 550 (1972).

Thomas, H. C., "Heterogeneous Ion Exchange in A Flowing System," *J. Am. Chem. Soc.*, **66**, 1664 (1944).

Wakao, N., and T. Funazkri, "Effect of Fluid Dispersion Coefficients on Particle-to-Fluid Mass Transfer Coefficients in Packed Bed," *Chem. Eng. Sci.*, **33**, 1375 (1978).

Walter, J. E., "Multiple Adsorption from Solutions," *J. Chem. Phys.*, **13**, 229 (1945a).

———, "Rate-Dependent Chromatographic Adsorption," *J. Chem. Phys.*, **13**, 332 (1945b).

Yang, R. T., S. J. Doong, and P. L. Cen, "Bulk Gas Separation of Binary and Ternary Mixtures by Pressure Swing Adsorption," *AIChE Symp. Ser.*, **81**, (242), 84 (1985).



*Manuscript received Oct. 31, 1985, and revision received Jan. 14, 1986.*